International Journal of Nanomedicine

Dovepress
open access to scientific and medical research

Open Access Full Text Article

ORIGINAL RESEARCH

Pioneering Astaxanthin-Tumor Cell Membrane Nanoparticles for Innovative Targeted Drug Delivery on Melanoma

Jui-Jen Chang[1,2,*], Yi-Chen Wang[3,4,*], Shu-Hui Yang[5,6], Ju-Yu Wu[7], Ming-Wei Chang[8], Hui-Min David Wang[5,9–11]

[1]Department of Medical Research, China Medical University Hospital, China Medical University, Taichung, 40447, Taiwan; [2]Graduate Institute of Integrated Medicine, China Medical University, Taichung, 40447, Taiwan; [3]Division of Cardiology, Department of Internal Medicine, Kaohsiung Armed Forces General Hospital, Kaohsiung City, 802, Taiwan; [4]Institute of Medical Science and Technology, National Sun Yat-sen University, Kaohsiung, 807, Taiwan; [5]Graduate Institute of Biomedical Engineering, National Chung Hsing University, Taichung, 402, Taiwan; [6]Bachelor Program of Biotechnology, National Chung Hsing University, Taichung, 402, Taiwan; [7]Doctoral Program in Tissue Engineering and Regenerative Medicine, National Chung Hsing University, Taichung, 402, Taiwan; [8]Nanotechnology and Integrated Bioengineering Centre, University of Ulster, Belfast, BT15 1AB, Northern Ireland, UK; [9]Graduate Institute of Medicine, College of Medicine, Kaohsiung Medical University, Kaohsiung, 807, Taiwan; [10]Department of Medical Laboratory Science and Biotechnology, China Medical University, Taichung, 404, Taiwan; [11]Center of Applied Nanomedicine, National Cheng Kung University, Tainan, 701, Taiwan

*These authors contributed equally to this work

Correspondence: Hui-Min David Wang, Graduate Institute of Biomedical Engineering, National Chung Hsing University, No. 145, Xingda Road, South Dist, Taichung City, 402, Taiwan, Tel +886-4-22840733#651; +886-935753718, Email davidw@dragon.nchu.edu.tw

Background: Recently, the use of the tumor or its secretions as drug carriers has gradually become popular, with the advantages of high biocompatibility and enhanced drug delivery to specific cells. Melanoma is the most malignant tumor of all skin cancers; it is the most metastatic and, therefore, the most difficult to treat. The main purpose of this study is to develop nanovesicles with tumor cell membrane secretion properties to encapsulate target substances to enhance the therapeutic effect of cancer.

Methods: Astaxanthin was selected as an anticancer drug due to our previous research finding that astaxanthin has extremely high antioxidant, anti-ultraviolet damage, and anti-tumor properties. The manufacturing method of the astaxanthin nanovesicle carrier is to mix melanoma cells and astaxanthin in an appropriate ratio and then remove the genetic material and inflammatory factors of cancer cells by extrusion.

Results: In terms of results, after the co-culture of astaxanthin nanovesicles and melanoma cancer cells, it was confirmed that the ability of astaxanthin nanovesicles to inhibit the growth and metastasis of melanoma cancer cells was significantly better than the same amount of astaxanthin alone, and it had no effect on normal Human cells are also effective. There was no apparent harm on normal cells, indicating the ability of the vesicles to be selectively transported.

Conclusion: Our findings illustrated the potential of astaxanthin nanovesicles as an anticancer drug.

Keywords: melanoma, astaxanthin, nanoparticle

Introduction

It is very difficult to detect melanoma at an early stage because the initial form of melanoma is no different from normal spots or moles on the skin. However, melanoma expands very fast over time, and a large number of uneven small round bumps will appear quickly on the patient's body.[1] The rapid deterioration, coupled with the poor effect of existing treatment drugs, and the high cost of treatment, make it easy for patients to ignore it and give up on treatment, resulting in mortality. It has the highest percentage among all skin cancer types. According to statistics from the Ministry of Health and Welfare, melanoma accounted for 60% of the overall skin cancer death rate in 2015. The current treatment methods for melanoma include surgery, chemotherapy, radiotherapy, and immunotherapy, but these treatments often cause strong side effects and cannot completely cure melanoma.[2,3] Modern methods use cell-targeting therapies. In nano-

Received: 9 September 2023
Accepted: 26 January 2024
Published: 7 March 2024

Graphical Abstract

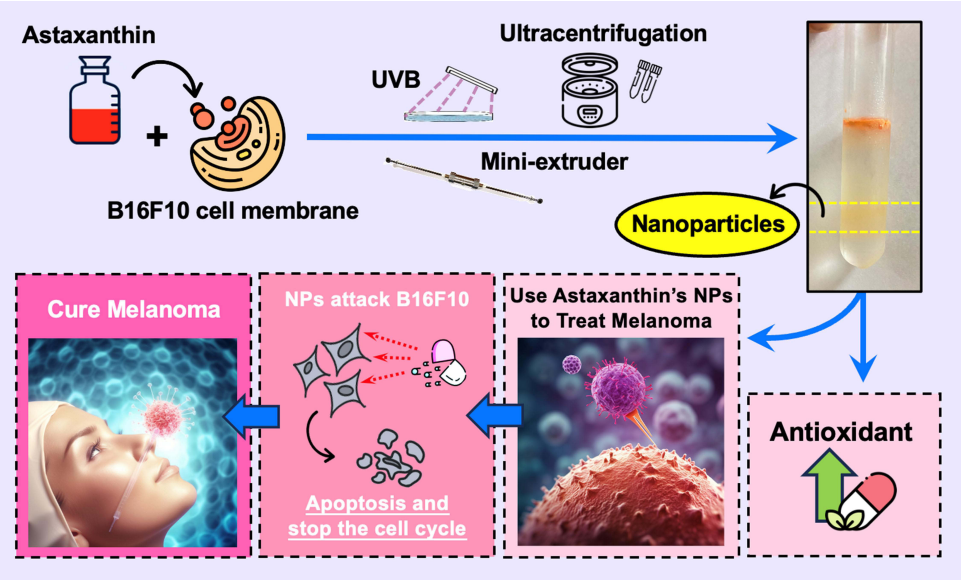

transportation technology, researchers will coat target drugs or proteins that promote tumor cell death into nano-drug carriers for treatment.[3–5] Relevant literature showed that making nanoscale particles from the cancer cell membrane has the potential to be used as a drug carrier, because nanoparticles have a structure similar to cell membranes (such as proteins, lipids, etc.), and can exhibit better biological properties.[6] Unlike naturally occurring extracellular vesicles such as exosomes and microvesicles, cell membrane-based nanovesicles are artificially fabricated. Moreover, cancer cells are more effectively targeted than other cells because of the properties of homotypic cell targeting.[6,7] Therefore, in this study we want to make nanoparticles from melanoma cancer cells, hoping that the nanoparticles can be attached and fused inside the melanoma cancer cells, to enhance the action of anticancer drugs and make the drugs more effective by directly targeting the cancer cells and destroy cancer cells.[8] In recent years, astaxanthin has been confirmed by various medical and biotechnology researchers to have excellent anti-oxidation, vision improvement, immunity enhancement, and even excellent anti-tumor abilities, a large number of related healthcare and nutrition products have gradually come into the market.[9–14] Hence, we decided to use astaxanthin as a precursor drug to inhibit melanoma and use melanoma cancer cells as nano-carriers, hoping to achieve the purpose of effective treatment of melanoma. Meanwhile, we have demonstrated through cell viability analysis that the vesicles we make are harmless to normal cells.

Materials and Methods

Materials

Astaxanthin, Phosphate Buffered Saline (PBS, Gibco), Dulbecco's Modified Eagle's Medium (DMEM, Gibco), CCK8 reagent kit (IMT Formosa Co., Ltd.), 1.1-diphenyl-2-picrylhydrazyl radical (DPPH, SIGMA), vitamin C, ethylenediaminetetraacetic acid (EDTA), butylated hydroxyl-anisole (BHA), Trichloroacetic acid (TCA), 2.2'-azino-bis (3-ethylbenzothiazoline-6-sulfonic acid)(ABTS, SIGMA), Potassium hexacyanoferrate(III), Bicinchoninic acid (BCA) protein assay kit (Pierce, Rockford, IL, USA), SYBR Green Master Mix (EntiLink^{TM}), Reverse transcription kit (Thermo Fisher).

Cell Lines

Melanoma carcinoma cells (B16F10), were purchased from the Bioresource Collection and Research Center (BCRC, Hsinchu, Taiwan). Skin fibroblasts (Hs68) were obtained from the American Type Culture Collection (ATCC, Manassas,

VA, USA; Hs68 Number: CRL-1635™). Lung Metastatic Melanoma (LMM) cells were based on the injection of B16F10 from the tail vein of mice and then extract the cancer cell from the lung after the tumor was built.

DPPH Free Radical Scavenging Assay

Astaxanthin 1.68 mM was prepared by dissolving in dimethyl sulfoxide (DMSO), then diluted as follows 1, 1/2, 1/4, 1/8, 1/12, and 1/24. The DPPH solvent is prepared by mixing 15 mg of DPPH powder and 15 mL of methanol solvent. 392 μL of DPPH solution was mixed with 8 μL of sample in a microcentrifuge tube, then 100 μL was taken to a 96-well plate and each sample was triplicated, finally, the absorbance was measured at 517 nm by using a spectrophotometer after 30 minutes in the dark. Compared with the absorbance value of the blank control group, the ability of each sample to scavenge free radicals can be judged. Moreover, vitamin C was used as the positive control group.[12]

ABTS Free Radical Scavenging Ability

Astaxanthin (1.68 mM) with DMSO as a solvent, dilute to 1, 1/2, 1/4, 1/8, 1/12, and 1/24 times the sample. The ABTS solution was prepared by mixing 180.11 mg of ABTS powder with 50 mL of deionized distilled water (ddH2O) solvent to form a 7 mM ABTS solution. Potassium persulfate solution was prepared by mixing 180.11 mg of potassium persulfate powder with 10 mL of ddH2O solvent to prepare a 140 mM potassium persulfate solution. 25 mL of ABTS solution was mixed with 440 μL of potassium persulfate solution to prepare $ABTS^{+}$ cationic radical solution. After keeping in the dark for 12 hours, the $ABTS^{+}$ cationic radical solution was diluted with ethanol until the absorbance value is 0.7 ± 0.002, then 20 μL of the sample was mixed evenly with 380 μL of $ABTS^{+}$ cationic radical solution and configured in a microcentrifuge tube, then 100 μL of the mixture was taken to the 96-well plate and the sample was triplicated, and the absorbance was measured at 734 nm by using a spectrophotometer after 30 minutes in the dark. Compared with the absorbance value of the blank control group, the ability of each sample to scavenge free radicals can be judged. Moreover, EDTA was used as the positive control group.[12]

Reducing Power Assay

Reagent configuration: take astaxanthin 1.68 mM with DMSO as solvent, and dilute to 1, 1/2, 1/4, 1/8, 1/12, 1/24 times. Experimental steps: prepare eight microcentrifuge tubes, add phosphate buffer 340 μL and red blood salt 7.5 μL into each microcentrifuge tube, take 7.5 μL of the above six samples into a microcentrifuge tube, and the other two microcentrifuge tubes were added butylated hydroxyl-anisole (BHA) and ddH2O 10 μL respectively as positive control and control group, eight microcentrifuges put the centrifuge tube in a water bath at 50 °C for 20 minutes, then put in ice cubes to cool down for 2 minutes, then add Trichloroacetic acid (TCA), put 160 μL into a microcentrifuge tube and centrifuge for 10 minutes (3,000 g). After centrifugation, take 75 μL of the supernatant to a 96-well plate with 3 repeats, and then add 25 μL $FeCl_3$ into a 96-well plate, and finally measure its absorbance with a spectrophotometer at 700 nm.[12]

Cryopreservation

Before freezing cells, a cell cryopreservation solution should be prepared, DMSO should be added to the fresh medium to make the final concentration 5–10%, mixed well, and placed at room temperature for use. According to the operation of cell subculture, collect the cells, and take a small amount of cell suspension to count the cell concentration and pre-freezing viability. Centrifuge the collected cells at 300 g for 5 minutes, remove the supernatant, add an appropriate amount of cryopreservation solution, mix well, make the cell concentration 1–5 × 10^6 cells / mL, and dispense into cryopreservation tubes. Dispense 1 mL per tube. Frozen storage in stages, placed at −20 °C for at least 20 minutes and put at −80 °C After about 16 hours, transfer to a liquid nitrogen tank for storage.[15]

Thawing

Prepare an empty petri dish and add 10 mL of culture medium (because the cell cryopreservation solution contains DMSO, it must be diluted 1:10), take out the cryovial to be thawed from the liquid nitrogen bucket, place the cell cryovial on the water bath (37 °C) for defrosting, then take out the cell solution, add it on the dish, put it in the incubator, and observe whether the cells adhere to the plate after a few hours.[15]

Subculture

Cell type: Melanoma cell (B16F10) / Lung Metastatic Melanoma (LMM) / fibroblasts (Hs68). Remove the original cell culture medium in the culture dish and rinse with PBS to remove the residual culture medium. After adding 1 mL of trypsin-EDTA to each culture dish, put it back into the incubator for about 7 minutes, and suspend the cells until it attached to the bottom of the dish. Add culture medium containing serum protein to terminate the action of trypsin-EDTA, and centrifuge at 360 g for 5 minutes. Remove the supernatant after centrifugation, add 2 mL of culture medium (DMEM) to redissolve, and mix well. Take out 1 mL of cell fluid put it in the dish and shake to make it evenly, and then put it back into the incubator. After a while, check again whether the cells have attached to the plate. The remaining cells can be mixed with cell cryopreservation solution and cell solution at a ratio of 1:1, then collected and stored in stages, kept at −20 °C for at least 20 minutes, and placed at −80 °C for about 16 hours, then moved to a liquid state Store in nitrogen tanks.[15]

Cell Viability Analysis (CCK8 Assay)

After reaching the light yellow WST8 (Water Soluble Tetrazolium 8) aqueous solution with the dehydrogenase in living cells, WST8 will be reduced to an orange formazan water-soluble product. Therefore, the number of viable cells is directly proportional to the shade of orange, and finally, the absorbance value is measured by a spectrophotometer at a wavelength of 450 nm to further obtain the survival ratio. Reagent configuration: take astaxanthin 1.68 mM and use DMEM as a solvent, dilute 1, 1/2, 1/4, 1/8, 1/12, 1/24 times the sample; and ANPs configured as 100, 125, 150, 175, and 200 μM. For the CCK8 reagent, take 10 μL of WST8 and dilute it 10 times with DMEM. Experimental procedure: Cells were cultured in 96-well plates for 24 hours. After that, they were incubated with astaxanthin solutions of different concentrations and DMEM, and then the cells were incubated at 37 °C for 24 hours in a 5% carbon dioxide environment. Finally, the WST8 solution was added to each well and incubated at 37 °C for 2 to 4 hours. Measur e the absorbance of the cell suspension at 450 nm using a spectrophotometer. The experiment was performed in triplicate and statistical analysis was performed to obtain the final values.[3]

Cell Scraping, Centrifugation, and Cell Count

Use sterile cell scrapers and add 1 mL of PBS to the melanoma cancer cells that have overgrown and attached to the wall of the cell culture dish, then scrape off and add to Eppendorf. Put Eppendorf into a centrifuge at 360 g for 10 minutes to allow the melanoma cancer cells to settle at the bottom of the centrifuge tube. Part of the melanoma cancer cells was mixed with PBS and dripped with trypan blue solution to distinguish live cells from dead cells, and the calculated number was estimated to obtain the total number of cells.[3]

Ultrasonic Vibration

Astaxanthin and cells were vibrated for 30 minutes by using ultrasonic. Due to the characteristics of high frequency, short wavelength, and strong penetrating power of ultrasonic waves, the extracted astaxanthin can be fully mixed and contacted with cells. After 30 minutes, pipette every 10 minutes for a total of 90 minutes.[3]

UVB Irradiation

The mixture of astaxanthin and melanoma cancer cells was transferred from the centrifuge tube to the culture medium, put into the instrument for irradiating UVB irradiation, and irradiated with UVB light for 2 minutes to destroy the DNA of melanoma cancer cells.[3]

Extrusion

First, the polycarbonate (PC) membrane with a pore size of 10 μm was put into the nano extruder, then squeeze the mixture of astaxanthin and melanoma cancer cells back and forth 5 times, and then repeating the above steps with a pore size of 5 μm's PC membrane. After the extrusion, the cell membrane of the cancer cells was extruded into nanoparticles to coat astaxanthin to fight against melanoma cancer cells.[3]

Ultra-High-Speed Centrifugation

A density gradient separation solution (60%) was added to the centrifuge tube, then nanoparticles were slowly added along the tube wall, and finally, the configure 10% density gradient separation solution was added so that the particles are located in the centrifuge tube's middle. Lock the configured centrifuge tube firmly in the ultracentrifuge, and set the ultracentrifuge to 100,000 g, 4 °C, for 2 hours. After centrifugation, the particles located in the center were pulled up and added to a 15 mL centrifuge tube.[3]

Cell Migration Assay (Migration Wound Healing Assay)

70 mL of B16F10 were added to the wound healing insert (Culture-Insert 2 Well) at 3×10^5 cells / mL per well and cultured for 24 hours. Afterward, the DMEM in the insert was pumped up and rinsed twice with PBS, and then cultured with different concentrations of particles and DMEM at 37 °C in an environment of 5% CO_2. After 16 hours, an optical microscope (Leica Microsystems) was used to photograph the degree of cell migration on the selected area using a 4× lens, and the area was calculated to obtain the cell migration rate.[3]

Dynamic Light Scattering (DLS) Particle Size Analysis

In this experiment, the particle size of the prepared sample was measured by the Litesizer. Litesizer is based on the principle of dynamic light scattering and photon spectrum to get the size of a particle according to the speed of the Brownian motion of the particle in the liquid. Due to the different movement rates in various sizes of the particle, different particles cause scattered light to scatter at different angles after being irradiated by laser. The acquired result was compared with the photon spectrum to obtain the size of the particle.[16]

Fluorescent Staining of Cells

The original cell culture medium in the culture dish was removed and rinsed with PBS to remove the residual culture medium. After 1 mL of trypsin-EDTA was added to each culture dish, put back into the incubator for about 7 minutes to allow the cell which attach/adhere to the bottom of the dish to suspend. Then, the culture medium containing serum protein was added to terminate the action of trypsin-EDTA and centrifuged at 360 g for 5 minutes. After centrifugation, the supernatant was removed, and add 2 mL of culture medium to re-dissolve and mixed well. 1 mL of Diluent C was added and mixed well with the cell solution; at the same time, 4 mL of PKH26 and 1 mL of Diluent C were taken, mixed in another centrifuge tube, the two tubes were mixed, and put in the incubator for 2–5 minutes, shake gently to make it even, then the same amount of serum was added, centrifuged for 400 g, 10 minutes. Then the supernatant was drained, re-dissolved by adding 1 mL of PBS and centrifuged, and repeated three times.[17]

Quantitative Real-Time Reverse Transcription Polymerase Chain Reaction (qRT-PCR) Analysis

The fluorescent signal was generated by a unique probe formed as qRT-PCR, which is a detection method using the StepOnePlusTM system (Thermo Fisher Scientific Inc., USA) fluorescence detection technology to sense each cycle. It detects and records the fluorescence intensity of each cycle and calculates real-time quantitative data. For the sample preparation, first used TRIzol (Invitrogen, Waltham, MA, USA) to extract RNA from LMM cells and then used a reverse transcription kit to generate cDNA. Add the SYBR Green Master Mix, templates, and primers. All steps were repeated for 40 amplification cycles, and the resultant was passed through the fluorescence detection system.[18] Primers for qRT-PCR are listed in Table S1.

Western Blotting

First prepared the SDS-PAGE gel, and test the sample with the BCA protein assay kit to calculate the protein's concentration. Run the SDS page with running buffer for 2 hours and transfer the gel with PVDF membrane in transfer buffer for one and a half hours. After the transfer process, use the blocking buffer and PBST wash for 5 minutes three times. Add the primary antibody to shake overnight, and then wash it with PBST before adding the second antibody.

West Femto Maximum Sensitivity Substrate Kit was used to visually detect the signal through enhanced chemiluminescence (ECL) detection.[18]

Research Results

Determination of Antioxidant Capacity

In this experiment, three different methods were used to test the antioxidant capacity of astaxanthin, including DPPH free radical scavenging assay, ABTS free radical scavenging ability, and reducing power assay. As shown in the DPPH free radical scavenging experiment (Figure 1a), Astaxanthin has DPPH free radical scavenging ability. In 0.07 mM astaxanthin, it only has about 15% DPPH free radical scavenging rate, while in 1.68 mM high-concentration astaxanthin, the DPPH scavenging ability is about 50%. At 0.42 and 0.84 mM, the antioxidant capacity is about 20%. Astaxanthin has a significant ability to scavenge ABTS free radicals (Figure 1b). At a low concentration of 0.07 mM astaxanthin, it has a free radical scavenging ability of 20%. When the concentration of astaxanthin is higher, the scavenging ability of ABTS free radicals also increases, with an obvious concentration trend; astaxanthin at higher concentrations of 0.42, 0.84, and 1.68 mM, the scavenging ability of ABTS free radicals was not significantly different from that of the positive control group, and the scavenging abilities of ABTS free radicals were all above 85%, showing strong antioxidant capacity. The experiment of reducing power measurement (Figure 1c), showed that astaxanthin had almost no reducing power to scavenge free radicals, and the reducing power of astaxanthin at each concentration is not significantly different from the control group. The DPPH and ABTS free radical scavenging ability of astaxanthin was measured by using IC_{50} (Figure 1d and e), and the IC_{50} of astaxanthin for scavenging ABTS was 0.28 mM (Figure 1e), It means that the

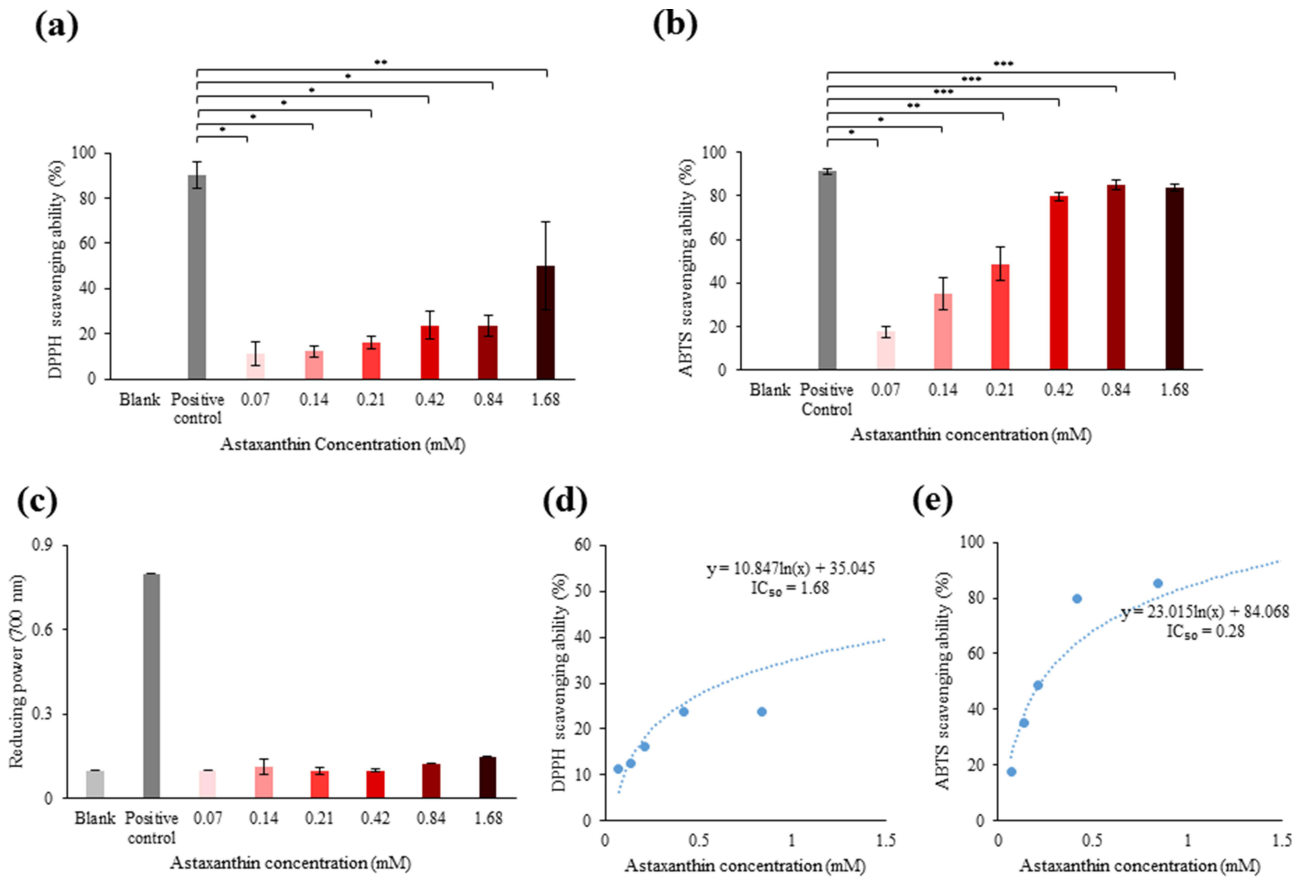

Figure 1 The antioxidant tests for astaxanthin. (**a**) The DPPH scavenging ability of astaxanthin. The blank control group was ddH_2O. The positive control group was 100 μM vitamin C. (**b**) The ABTS scavenging ability of astaxanthin. The blank control group was ddH2O. The positive control group was EDTA. (**c**) The reducing power of astaxanthin. The blank control group was ddH_2O. The positive control was BHA. (**d**) The IC_{50} of DPPH scavenging ability in astaxanthin. (**e**) The IC_{50} of ABTS scavenging ability in astaxanthin. *P < 0.05; **P < 0.01; ***P < 0.005 vs the control group.

antioxidant capacity of astaxanthin reaches 50% when the concentration is 0.28 mM; while the IC_{50} of DPPH free radical scavenging rate is about 1.68 mM (Figure 1d). Based on the above results, it can be proved that astaxanthin does have the extremely efficient antioxidant capacity, and has better performance in scavenging DPPH and ABTS free radicals. Astaxanthin exhibited excellent ABTS antioxidant capacity at concentrations of 0.4, 0.84, and 1.68 mM, which had no significant difference from the positive control group. Therefore, we selected 0.42 and 0.84 mM astaxanthin for subsequent experiments. It was found that astaxanthin can unbalance intracellular free radicals and antioxidants, so it can give cancer cells more oxidative stress to inhibit their growth.[19]

Nanoparticle Size Analysis and Protein Quantification

DLS Particle Size Analysis

After astaxanthin's antioxidant capacity determination, the antioxidant capacity of 0.42 and 0.84 mM astaxanthin is better. Therefore, two different concentrations of astaxanthin (0.42 and 0.84 mM) were mixed with melanoma cancer cells to produce two different ANPs. One was coated with 0.42 mM astaxanthin, and the other was 0.84 mM (Figure 2a). ANPs (0.42 mM) are about 470 nm in diameter nm and ANPs (0.84 mM) are about 1,620 nm in diameter.

Bicinchoninic Acid Assay (BCA)

After making a standard curve for the BCA protein, measure it with a spectrophotometer, and then detect the absorbance value of the melanoma cancer cells. Then substitute the obtained data into the standard curve to obtain the protein concentration of melanoma cancer cells as 1.4 mg / mL. And use the same method to measure ANPs (0.42 and 0.84 mM), the values measured by the spectrophotometer were brought into the standard curve for calculation, and the protein contents of ANPs (0.42 and 0.84 mM) were about 0.48 and 0.77 mg / mL. This experiment shows that the larger the size of the ANPs, the higher the protein concentration it contains (Figure 2b).

Cell Viability Analysis

This experiment was divided into three parts, and the purpose was to detect ANPs (0.42 and 0.84 mM) have the ability to fight against melanoma cancer cells and whether the nanoparticles have a tendency of selective transport. In the first part of the experiment, the astaxanthin was not coated within nanoparticles to analyze the viability of B16F10 cells. As shown in Figure 3a, the concentration of uncoated astaxanthin was 50–1,000 μM, and the survival rate of melanoma cancer cells dropped from 70% at 150 μM to less than 20% at 175 μM. It was shown that uncoated astaxanthin had a half-lethal effect between 150 and 175 μM. It has also been confirmed that astaxanthin has the function of anti-melanoma and has the potential as an anticancer drug. Therefore, in the next experiment, to determine the anti-cancer properties of ANPs, we selected 100, 125, 150, 175, and 200 μM astaxanthin for follow-up experiments. The second part of the experiment compared the effects within and uncoated nanoparticles of astaxanthin on the survival rate of B16F10. The results proved that ANPs enhanced the ability of astaxanthin's resistance to cancer effect (Figure 3b). Since astaxanthin is encapsulated in nanoparticles, the effective concentration of astaxanthin will change after the astaxanthin is encapsulated in

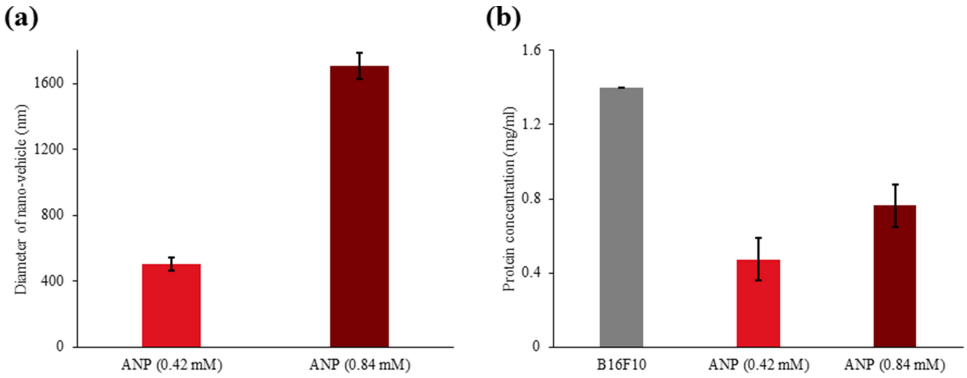

Figure 2 The particle property analysis. (**a**) The dynamic light scattering (DLS) particle size analyzer managed the size of ANPs. (**b**) The protein concentration of the ANPs.

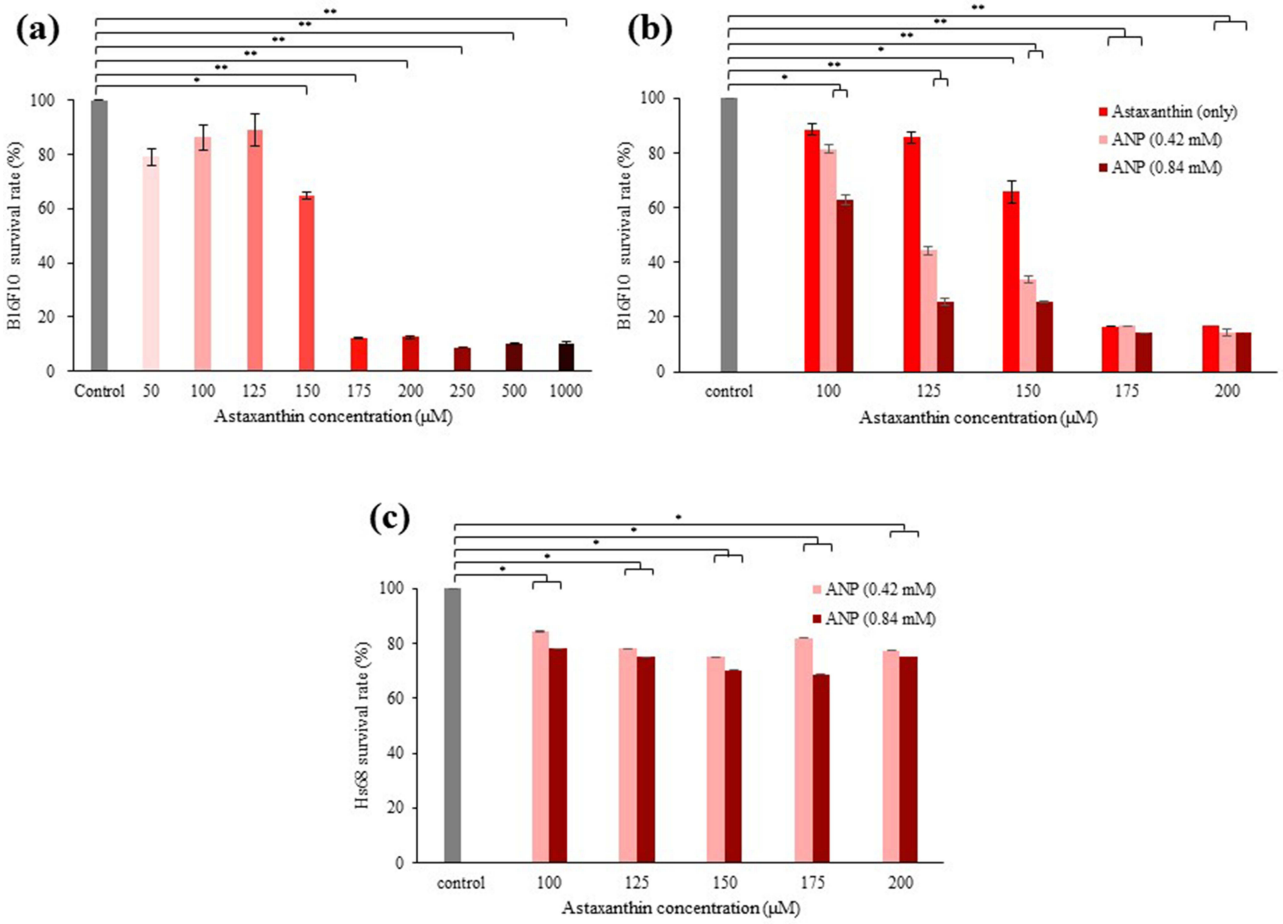

Figure 3 Cell survival rate. (**a**) The cell survival rate in B16F10 after conducting different concentrations of uncoated astaxanthin. (**b**) The cell survival rate in B16F10 after conducting different concentrations of astaxanthin and ANPs (0.42 and 0.84 mM). (**c**) The cell survival rate in Hs68 after conducting different concentrations of ANPs (0.42 and 0.84 mM). *P < 0.05; **P < 0.01 vs the control group.

nanoparticles. Therefore, we used the calibration curve of astaxanthin concentration to calculate the assay concentrations of ANPs (0.42 and 0.84 mM) to compare astaxanthin concentrations in NPs with uncoated. Calculate the detected concentration 100, 125, 150, 175, and 200 μM of ANPs (0.42 and 0.84 mM), and the comparison of cell viability experiments with uncoated astaxanthin (Figure 3b). In the uncoated astaxanthin group, the mortality rate of B16F10 was consistent with the values, 150 μM astaxanthin had a 70% survival rate, and 175 and 200 μM astaxanthin had a survival rate below 20%. At 100–150 μM, the ANPs have strong cytotoxicity of B16F10 cells. For example, at 125 μM, the rate of the uncoated group's B16F10 was higher than 80%, which was not significantly different from that of the control group; however, the survival rate of B16F10 with ANPs (0.42 mM) decreased significantly about 40%; the cell survival rate of ANPs (0.84 mM) was only 20%. Although the cell viability of uncoated astaxanthin and ANPs (0.42 and 0.84 mM) at concentrations of 175 and 200 μM did not show a significant difference, but still with a tendency for cell viability to be lower than the uncoated group. The results of this experiment show that astaxanthin has a better ability to inhibit cancer cells in the case of coating nanoparticles, and the higher the concentration of ANPs, the greater the ability to inhibit cell survival. The third part of the experiment will test whether the nanoparticles have the ability to inhibit other non-melanoma cells, that is, whether the nanoparticles have the tendency to deliver drugs to specific cells (Figure 3c). The experiment used the cell viability of Hs68 under the treatment of ANPs (0.42 and 0.84 mM). In the experiment (Figure 3c), there was no significant difference in the survival rate of Hs68 between 100–200 μM ANPs (0.42 and 0.84 mM), and the survival rate was above 70%, although ANPs(0.84 mM) was slightly better than ANPs (0.42 mM) in

suppressing tumor efficiency, there was still no significant difference. This experiment proves that our nanoparticles indeed tend to deliver drugs to specific cells.

Fluorescent Staining of Cells

In this experiment, we first stained the outer membrane of ANPs (0.42 and 0.84 mM) with PKH 26 fluorescent dye, then cultured the stained ANPs with cells for one day, and observed them with a microscope to determine whether ANPs were taken into cells. ANPs were used as the drug. Used the cell types of B16F10 in normal culture, as a control group. The experimental group was prestained ANPs (0.42 and 0.84 mM), adding to B16F10 (Figure 4a and b). In Figure 4a and b, it can be found that ANPs (0.42 and 0.84 mM) in B16F10 both emit red fluorescence in the cell, and on the second day, a lot of cellular debris was found in the photo of the experiment. This proves that ANPs can indeed enter cells and can effectively inhibit the growth of B16F10. Based on the above results, it can be confirmed that ANPs can efficiently enter B16F10 to inhibit cell growth and cause cell death.

Mobility Analysis

This experiment observes whether ANPs can effectively inhibit the migration of B16F10. The experimental group was ANPs (0.42 and 0.84 mM) (Figure 5), which were diluted to 200, 175, 150, 125, and 100 μM; the control group was normal cell after culture 16 hours, compared with the control group, it was found that ANPs (0.84 mM) can effectively inhibit the proliferation and growth of cancer cells at concentrations of 200 and 150 μM. While among ANPs (0.42 mM), the concentrations of 200, 175, and 125 μM showed excellent inhibition performance, and at the concentration of 125 μM, a small part of cell death was observed. However, 20 hours after the drug was administered, a large number of cells died suddenly, which may be due to the ANPs targeting cancer cells with a very strong poisoning rate. In summary, it was verified that ANPs can effectively inhibit metastasis and migration of cancer cells.

qRT-PCR & Western Blotting

We used the ANPs (0.84 mM) and LMM to co-culture for one day before performing qRT-PCR. We chose the genes related to apoptosis, including p21, p27, Bax, and Bcl-2. Some studies prove that p21 can regulate the cell cycle, induce apoptosis, and inhibit cell proliferation, and p27 can inhibit cyclin-CDK to arrest the cell cycle.[19,20] Bcl-2 is an antiapoptotic protein that can suppress apoptosis. Some studies have shown that Bcl-2 could suppress apoptosis by interacting with Bax.[21] Bax is a member of the Bcl-2 gene family, which is regulated by the tumor suppressor p53 and involved in p53-mediated apoptosis. So, we chose this gene to test the effect of the nanoparticles. The results showed that our ANPs can induce apoptosis and stop the LMM's cell cycle. It proves that ANPs can successfully induce melanoma cells (Figure 6a). And we also used ANPs with a concentration of 0.84 mM and LMM cells to co-culture for one day, and then do the Western blot to detect the expression of the same genes as in qRT-PCR detection. The results were similar to the qRT-PCR, confirming that ANPs could induce the apoptosis of LMM and can stop its cell cycle (Figure 6b).

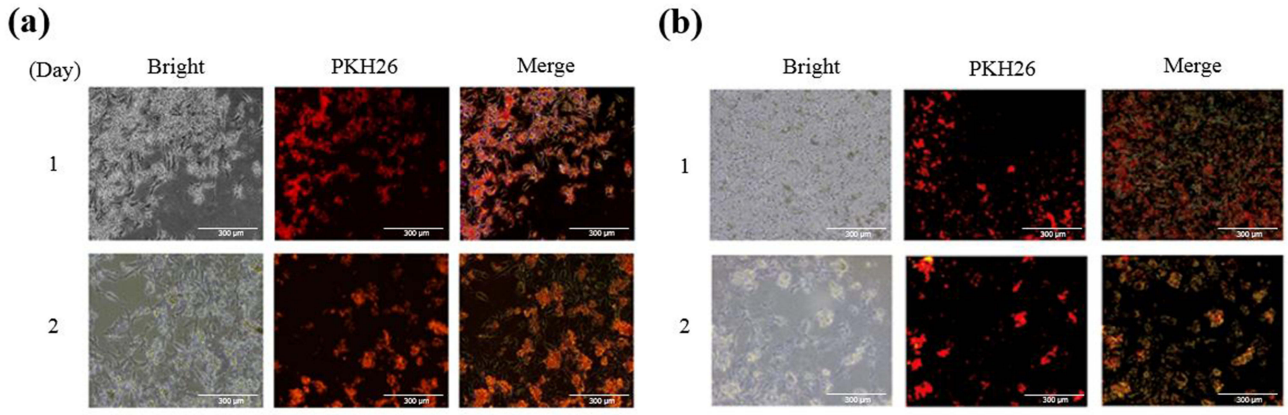

Figure 4 Fluorescent staining of cells under the field of 40× magnification. (**a** and **b**) The B16F10 was co-incubated for 24 hours with PKH26-stained ANPs (0.42 and 0.84 mM).

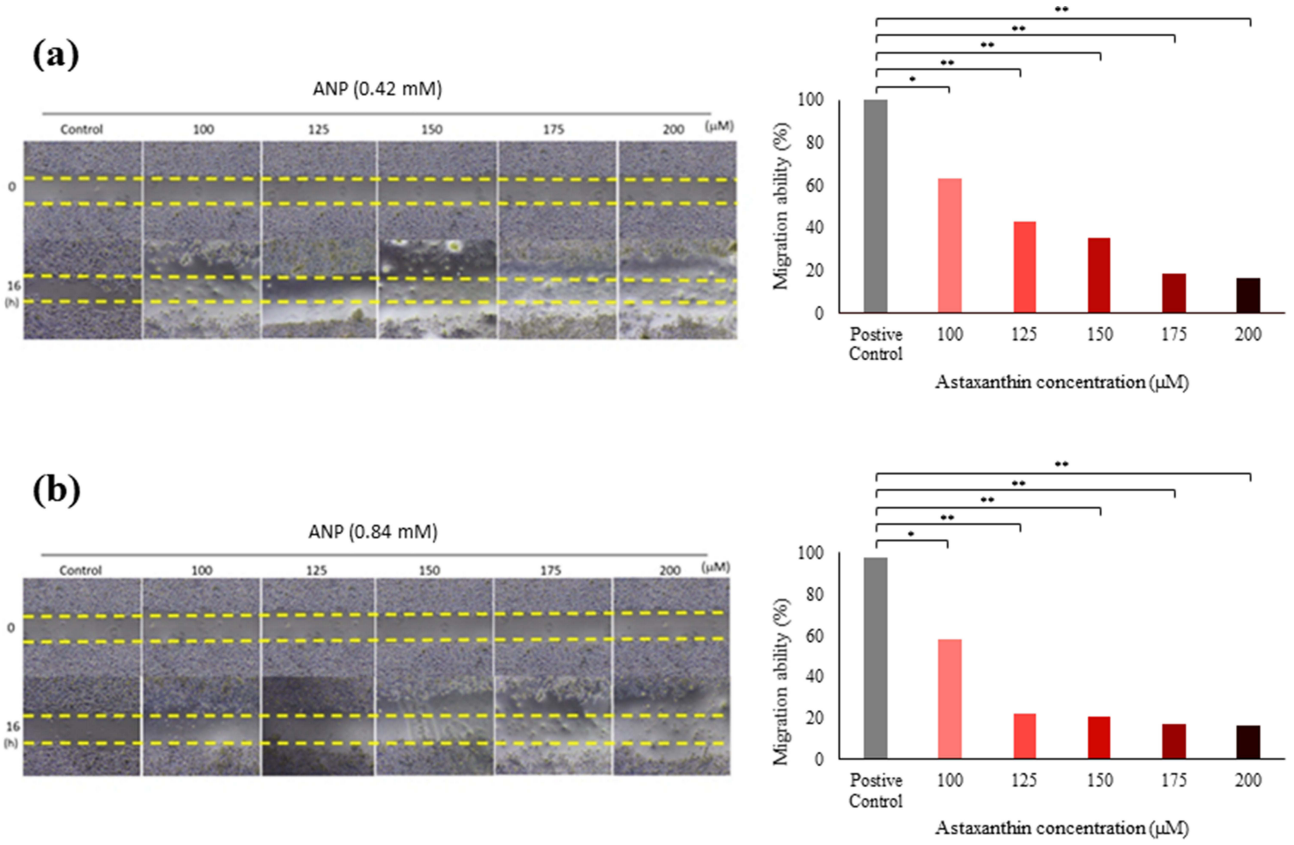

Figure 5 Migration assay of melanoma cancer cells. (**a**) Cell morphology of melanoma carcinoma cells cultured with ANPs (0.42 mM) for 16 hours and migration rate of melanoma cancer cells. (**b**) Cell morphology of melanoma carcinoma cells cultured with ANPs (0.84 mM) for 16 hours and migration rate of melanoma cancer cells. Samples vs control: *P < 0.05; **P < 0.01.

Discussion

First of all, in the antioxidant ability experiment, we have done three experiments to prove that astaxanthin has excellent antioxidant ability, DPPH, ABTS, and Reducing power. The experimental data of DPPH and ABTS showed that the higher the concentration of astaxanthin, the better its ability to scavenge free radicals. This proves that astaxanthin has a strong antioxidant capacity, consistent with the experimental results in the literature we consulted.[9,10] In the cell migration experiment, astaxanthin was co-cultured with melanoma cancer cells, which proved that astaxanthin can effectively inhibit the migration and spread of melanoma cancer cells. The experiment found that the higher the concentration of ANPs, the more effectively the melanoma cancer cells' growth is inhibited. After searching the literature, it was found that astaxanthin can unbalance intracellular free radicals and antioxidants, so it can give cancer cells more oxidative stress to inhibit their growth.[22]

In manufacturing nanoparticles, BCA protein measurement, and DLS particle size analysis were used as the experimental basis to confirm the properties of ANPs. In the BCA protein assay experiment, we confirmed that some proteins on the ANPs came from the original melanoma cancer cells themselves, and after measurement, they were compared with the original protein content (1.4 mg / mL), ANPs 0.42 and 0.84 mM were 35 and 60%. In the DLS particle size analysis experiment, it was confirmed that the self-made ANPs are indeed nanoscale carriers, with a size between 400 and 1,600 nm, resulting in a large difference in the size of ANPs (0.42 and 0.84 mM). This is because the similar substances of the protein produce clustering and adhesion effects, resulting in the size of ANPs (0.84 mM) being about two times that of ANPs (0.42 mM). Generally, the size of exosomes is between 50 and 200 nm. Although the volume of the particles produced is about twice as large as that of exosomes, they are still at the nanometer level. This feature provides a larger drug surface area in contact with the cells and greatly increases the cells' absorption of drugs in the particles. Moreover, in terms of protein yield, the literature demonstrates that cell membrane vesicles have an advantage over exosomes.[23]

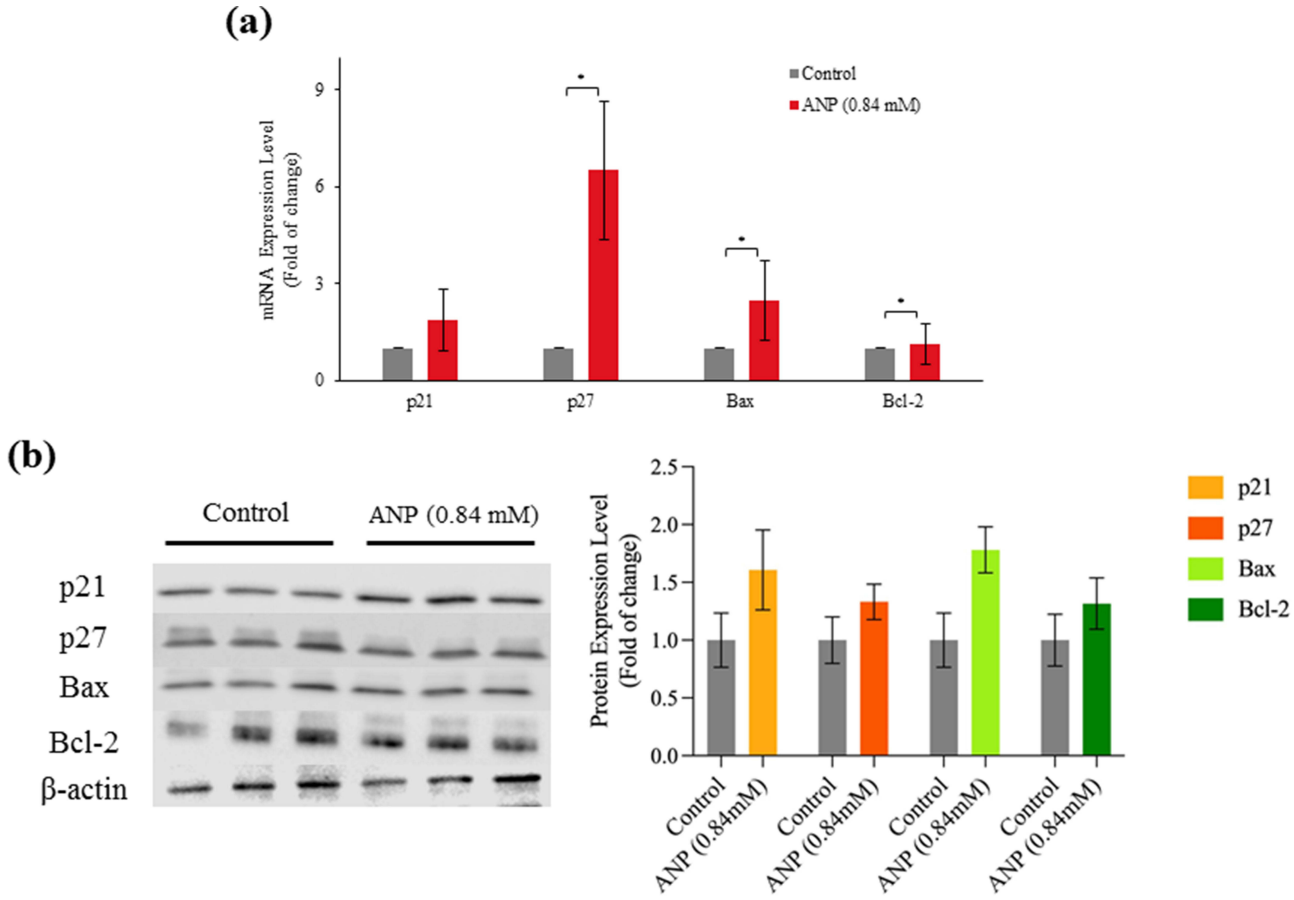

Figure 6 qRT-PCR Analysis and Western blotting (**a**) q-PCR test of ANPs (0.84 mM). *P < 0.05 (**b**) Western blot test of ANPs (0.84 mM).

To test whether ANPs can inhibit the growth of melanoma cancer cells. We tested the cell viability of different concentrations of astaxanthin solution and ANPs. The results showed that the death rate of melanoma was higher in the case of nanoparticle coating. This experiment demonstrates that the use of nanoparticles as drug carriers may have the potential to enhance drug effects. In addition, we wanted to know whether ANPs also had inhibitory properties on non-melanoma cancer cells. So we also tested the survival rate of fibroblasts (Hs68). In the data, it was confirmed that Hs68 had less acceptance of astaxanthin, and the cell viability was almost above 70%. This result represents that ANPs will not significantly reduce the survival rate of other cells and kill normal cells, but it has a very high lethal rate for melanoma cancer cells. This result represents that ANPs have a certain degree of cell specificity. Furthermore, through cell migration experiments, it can be observed that ANPs can inhibit the growth of cancer cells within 16 to 18 hours, and cause cell apoptosis after 24 hours, confirming that ANPs can effectively inhibit the metastasis and migration of cancer cells; and through fluorescent staining, it can be observed that the fluorescent dye had entered into melanoma cancer cells, but not into normal cells (Figure S1), which means that we used the melanoma cells themselves to make nanoparticles can be fused with normal melanoma cancer cells, and the astaxanthin drug-coated in the particles can be directly sent into melanoma cancer cells, and it can also be observed from the fluorescent picture. The complete coverage of the stained ANPs around the melanoma cancer cells further confirmed the better absorption of nanomedicines. This was not the case for other cells. Some studies have shown that certain cell markers (CD protein) and integrins (integrin) on the cell membrane (nanoparticle membrane) are unique to melanoma cancer cells.[24] Therefore, this experiment showed the specificity of nanoparticle drug delivery. The qRT-PCR and Western blotting results indicate an upregulation trend in the expression of apoptosis-related genes when melanoma cells are co-cultured with ANPs. This suggests that ANPs successfully induce melanoma cells, leading to a halt in the cell cycle.

In recent years, the application of targeted therapy and immunotherapy has significantly enhanced survival rates in advanced melanoma patients, particularly those with BRAF gene mutations.[25] Notably, checkpoint inhibitors like Pembrolizumab, approved by the US Food and Drug Administration (FDA), have demonstrated a five-year overall survival rate of 43.3%.[26] Despite these advancements, the challenge of drug resistance persists. The intricate components of the tumor microenvironment (TME) contribute to drug resistance, influencing cancer progression and impacting survival rates.[27]

Conclusions

These experiments have proved that astaxanthin has excellent antioxidant capacity, especially in the performance of ABTS and DPPH free radical scavenging rate. In the part of the confirmation of the characteristics of nanoparticles. The BCA protein assay showed that the composition of nanoparticles is not only the phospholipid composition of the cell membrane but also protein.

Our research proved ANPs have a better effect of inhibiting the growth of melanoma, which can enhance the effect of cancer drugs but did not affect the cell viability of Hs68. Furthermore, it was confirmed that ANPs have the tendency to deliver drugs to specific cells and they can effectively inhibit the migration ability of cancer cells, induce apoptosis, and stop the cell cycle of B16F10. Based on the above results, hope the nanoparticle we made could lead to new therapeutic approaches in the treatment of melanoma.

Acknowledgment

This manuscript is thanks to the experiment assistances from Shih-jyun Huang, Zong-Ren Jiang, Yi-Siang Chen (Taichung Second Senior High School), and Liang-Fang Lin (National Chung Hsing University). The authors also acknowledge the support from the Center of AppliedNanomedicine at National Cheng Kung University from The Featured Areas ResearchCenter Program within the framework of the Higher Education Sprout Project bythe Ministry of Education.

Funding

This research was supported by National Science and Technology Council, Taiwan under grant nos. NSTC 111-2221-E-005-026-MY3, 111-2221-E-005-009, MOST 110-2221-E-039-002-MY3 and 110-2221-E-029-005. This work was also supported by Kaohsiung Armed Forces General Hospital (KAFGH_D_112027).

Disclosure

The authors declare that they have no known competing financial interests or personal relationships that could have appeared to influence the work reported in this paper.

References

1. Dzwierzynski WW. Melanoma risk factors and prevention. *Clin Plast Surg*. 2021;48(4):543–550. doi:10.1016/j.cps.2021.05.001
2. Ahmed B, Qadir MI, Ghafoor S. Malignant melanoma: skin cancer-diagnosis, prevention, and treatment. *Crit Rev Eukary Gene Expres*. 2020;30(4):291–297. doi:10.1615/CritRevEukaryotGeneExpr.2020028454
3. Lin YY, Chen CY, Ma DL, Leung CH, Chang CY, Wang HMD. Cell-derived artificial nanovesicle as a drug delivery system for malignant melanoma treatment. *Bio Pharmacoth*. 2022;147:112586. doi:10.1016/j.biopha.2021.112586
4. Cheng YC, Chang YA, Chen YJ, et al. The roles of extracellular vesicles in malignant melanoma. *Cells*. 2021;10(10):2740. doi:10.3390/cells10102740
5. Haung HY, Wang YC, Cheng YC, et al. A novel oral astaxanthin nanoemulsion from Haematococcus pluvialis induces apoptosis in lung metastatic melanoma. *Oxid Med Cell Longev*. 2020;2020:2647670. doi:10.1155/2020/2647670
6. Le QV, Lee J, Lee H, Shim G, Oh YK. Cell membrane-derived vesicles for delivery of therapeutic agents. *Acta Pharmaceutica Sinica B*. 2021;11(8):2096–2113. doi:10.1016/j.apsb.2021.01.020
7. Cai JX, Liu JH, Wu JY, et al. Hybrid cell membrane-functionalized biomimetic nanoparticles for targeted therapy of osteosarcoma. *Int j Nanomed*. 2022;2022:837–854. doi:10.2147/IJN.S346685
8. Prajapat VM, Mahajan S, Paul PG, et al. Nanomedicine: a pragmatic approach for tackling melanoma skin cancer. *J Drug Delivery Sci Technol*. 2023;104394. doi:10.1016/j.jddst.2023.104394
9. Chou HY, Lee C, Pan JL, et al. Enriched astaxanthin extract from Haematococcus pluvialis augments growth factor secretions to increase cell proliferation and induces MMP1 degradation to enhance collagen production in human dermal fibroblasts. *Int J Mol Sci*. 2016;17(6):955. doi:10.3390/ijms17060955
10. Chen YT, Kao CJ, Huang HY, et al. Astaxanthin reduces MMP expressions, suppresses cancer cell migrations, and triggers apoptotic caspases of in vitro and in vivo models in melanoma. *J Funct Foods*. 2017;31:20–31. doi:10.1016/j.jff.2017.01.005

11. Tseng CC, Lin YJ, Liu W, et al. Metabolic engineering probiotic yeast produces 3S, 3'S-astaxanthin to inhibit B16F10 metastasis. *Food Chem Toxicol*. 2020;135:110993. doi:10.1016/j.fct.2019.110993
12. Samuel SY, Wang HMD, Huang MY, et al. Safety Assessment of 3S, 3'S astaxanthin derived from metabolically engineered K. marxianus. *Antioxidants*. 2022;11(11):2288. doi:10.3390/antiox11112288
13. Chou HY, Ma DL, Leung CH, Chiu CC, Hour TC, Wang HMD. Purified astaxanthin from Haematococcus pluvialis promotes tissue regeneration by reducing oxidative stress and the secretion of collagen in vitro and in vivo. *Oxid Med Cell Longev*. 2020;2020:4946902. doi:10.1155/2020/4946902
14. Donoso A, González-Durán J, Muñoz AA, González PA, Agurto-Muñoz C. Therapeutic uses of natural astaxanthin: an evidence-based review focused on human clinical trials. *Pharmacol Res*. 2021;166:105479 doi:10.1016/j.phrs.2021.105479.
15. Chou HY, Liu LH, Chen CY, et al. Bifunctional mechanisms of autophagy and apoptosis regulations in melanoma from Bacillus subtilis natto fermentation extract. *Food and Chemical Toxicology*. 2021;150:112020. doi:10.1016/j.fct.2021.112020
16. Huang SJ, Wang TH, Chou YH, et al. Hybrid PEGylated chitosan/PLGA nanoparticles designed as pH-responsive vehicles to promote intracellular drug delivery and cancer chemotherapy. *Int J Biol Macromol*. 2022;210:565–578. doi:10.1016/j.ijbiomac.2022.04.209
17. Cheng YS, Yen HH, Chang CY, et al. Adipose-derived stem cell-incubated HA-rich sponge matrix implant modulates oxidative stress to enhance VEGF and TGF-β secretions for extracellular matrix reconstruction in vivo. *Oxid Med Cell Longev*. 2022;2022:1–17. doi:10.1155/2022/9355692
18. Lan YH, Lu YS, Wu JY, et al. Cordyceps militaris reduces oxidative stress and regulates immune T cells to inhibit metastatic melanoma invasion. *Antioxidants*. 2022;11(8):1502. doi:10.3390/antiox11081502
19. Fu T, Liang A, Liu Y. Role of P21 in resistance of lung cancer. *Zhongguo fei ai za zhi*. 2020;23(7):597–602. doi:10.3779/j.issn.1009-3419.2020.101.16
20. Razavipour SF, Harikumar KB, Slingerland JM. p27 as a transcriptional regulator: new roles in development and cancer. *Cancer Res*. 2020;80 (17):3451–3458. doi:10.1158/0008-5472.CAN-19-3663
21. Li J, Chen CY, Huang JY, et al. Isokotomolide a from Cinnamomum kotoense induce melanoma autophagy and apoptosis in vivo and in vitro. *Oxid Med Cell Longev*. 2020;2020:3425147. doi:10.1155/2020/3425147
22. Hien HTM, Oanh HT, Quynh QT, et al. Astaxanthin-loaded nanoparticles enhance its cell uptake, antioxidant and hypolipidemic activities in multiple cell lines. *J Drug Deliv Sci Technol*. 2023;80:104133. doi:10.1016/j.jddst.2022.104133
23. Xu C, Ju D, Zhang X. Cell membrane-derived vesicle: a novel vehicle for cancer immunotherapy. *Front Immunol*. 2022;13:923598. doi:10.3389/fimmu.2022.923598
24. Vaníčková L, Do T, Vejvodová M, et al. Mapping of MeLiM melanoma combining ICP-MS and MALDI-MSI methods. *Int J Biol Macromol*. 2022;203:583–592. doi:10.1016/j.ijbiomac.2022.01.139
25. Jenkins RW, Fisher DE. Treatment of advanced melanoma in 2020 and beyond. *J Invest Dermatol*. 2021;141(1):23–31. doi:10.1016/j.jid.2020.03.943
26. Long GV, Schachter J, Arance A, et al. Long-term survival from pembrolizumab (pembro) completion and pembro retreatment: Phase III KEYNOTE-006 in advanced melanoma. *Am Soc Clin Oncol*. 2020;38:10013. doi:10.1200/JCO.2020.38.15_suppl.10013
27. Khalaf K, Hana D, Chou JTT, Singh C, Mackiewicz A, Kaczmarek M. Aspects of the tumor microenvironment involved in immune resistance and drug resistance. *Front Immunol*. 2021;12(12):656364. doi:10.3389/fimmu.2021.656364